Theoretical Studies on Models for the Oxo-Transfer Reaction of Dioxomolybdenum Enzymes

Michelle A. Pietsch and Michael B. Hall*

Department of Chemistry, Texas A&M University, College Station, Texas 77843-3244

Received August 9, 1995[⊗]

Patterned after synthetic model systems for dioxomolybdenum enzymes, our theoretical model system produces an energy profile and structures for the various species and oxidation states in the catalytic cycle. A key step in this cycle is the oxo-transfer reaction. Here, our substrate, PMe_3, approaches $[Mo^{VI}O_2]^{2+}$ at an O−Mo−O−P dihedral angle of 90°, i.e. perpendicular to the MoO_2 plane, crosses over a barrier of 14 kcal/mol, and rotates to an O−Mo−O−P dihedral angle of 0° to form an intermediate, $[Mo^{IV}O(OPMe_3)]^{2+}$, which is 69 kcal/mol more stable than the reactants. The direction of the substrate's attack leaves the two d electrons of this Mo(IV) system in an orbital which is δ with respect to the remaining spectator Mo−O bond, a configuration which allows this O to form a formal triple Mo−O bond. The displacement of the product, OPR_3, by water, H_2O, proceeds via an associative mechanism with a barrier of only 19 kcal/mol. In our model, $[Mo^{IV}O(OH_2)]^{2+}$ then reacts with $[Mo^{VI}O_2]^{2+}$ to form $[Mo^{V}O(OH)]^{2+}$, a process which is exothermic by 14 kcal/mol. The addition of O_2 then oxidizes $[Mo^{V}O(OH)]^{2+}$ to $[Mo^{VI}O_2]^{2+}$ to complete our model catalytic cycle.

Introduction

A number of well-known enzymes, including xanthine oxidase, nitrate reductase, and sulfite oxidase, contain a similar molybdenum center.[1] For these molybdenum enzymes, it is believed that one or two oxo groups and two or three sulfur groups are present but the complete stereochemistry is still unknown.[1] Since these enzymes catalyze the transfer of an oxygen atom to and from a substrate, they are termed oxotransferases.[1−3]

The simplest catalytic cycle that incorporates the known physical and chemical properties of the oxotransferases is shown in Scheme 1.[4] With the addition of a substrate, X, and H_2O, $[Mo^{VI}O_2]^{2+}$ is reduced to $[Mo^{IV}O(OH_2)]^{2+}$ and a substrate oxide, XO, is formed. By one-electron processes, $[Mo^{IV}O(OH_2)]^{2+}$ is first oxidized to $[Mo^{V}O(OH)]^{2+}$, which is then oxidized back to $[Mo^{VI}O_2]^{2+}$.

A number of Mo(VI) and Mo(IV) complexes have been synthesized to model the oxo−molybdenum enzymes.[1−5] These complexes range from having four monodentate ligands[6] to having a single tetradentate ligand[7] attached to the molybdenum center. With the ability to synthesize Mo(VI) and Mo(IV) species readily, many experimental groups have studied the first step of the catalytic cycle, known as an oxo-transfer reaction.[8,9]

Scheme 1

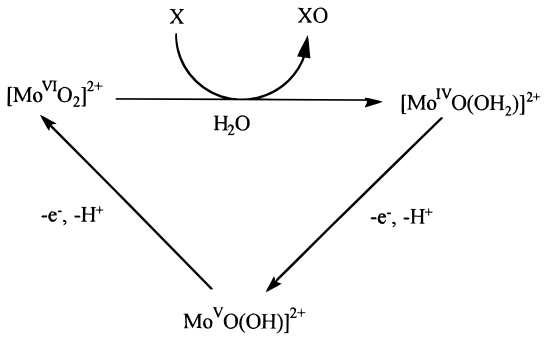

Scheme 2

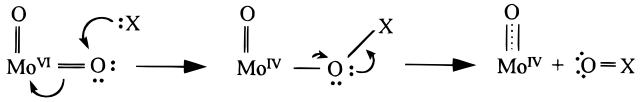

Recently, Schultz and Holm[9] completed the most comprehensive study on the reverse oxo-transfer reaction. Each substrate oxide, XO, was reduced with $Mo^{IV}O(^tBuL\text{-}NS)_2$ (^{t}BuL-NS is bis(4-*tert*-butylphenyl)-2-pyridylmethanethiolate(1−)) to form X and $Mo^{VI}O_2(^tBuL\text{-}NS)_2$. For each substrate, the reaction exhibited well-behaved second-order kinetics and had relatively large negative activation entropy, which indicates an associative transition state. Schultz and Holm concluded that it was very plausible that a transition state or intermediate exists with the substrate oxide attached to $Mo^{IV}O(^tBuL\text{-}NS)_2$, i.e. $Mo^{IV}O(OX)(^tBuL\text{-}NS)_2$.

Scheme 2 shows one possible mechanism for the oxo-transfer step in the forward direction.[3] The substrate, X, approaches an oxygen of the Mo(VI) species, forming a substrate−oxygen σ bond. The transfer of the molybdenum−oxygen π bonding electrons to the metal center weakens the molybdenum−oxygen bond, and the oxygen atom breaks from the molybdenum, forming the Mo(IV) species and OX.

[⊗] Abstract published in *Advance ACS Abstracts,* February 1, 1996.

(1) Enemark, J. H.; Young, C. G. *Adv. Inorg. Chem.* **1993**, *40*, 1.
(2) Holm, R. H. *Chem. Rev.* **1987**, *87*, 1401.
(3) Holm, R. H.; Berg, J. M. *Acc. Chem. Res.* **1986**, *19*, 363
(4) Xiao, Z.; Young, C. G.; Enemark, J. H.; Wedd, A. G. *J. Am. Chem. Soc.* **1992**, *114*, 9194.
(5) Das, S. K.; Chaudhury, P. K.; Biswas, D.; Sarkar, S. *J. Am. Chem. Soc.* **1994**, *116*, 9061. Barbaro, P.; Bianchini, C.; Scapacci, G.; Masi, D.; Zanello, P. *Inorg. Chem.* **1994**, *33*, 3180. Caradonna, J. P.; Reddy, P. R.; Holm, R. H. *J. Am. Chem. Soc.* **1988**, *110*, 2139.
(6) Arzoumanian, H.; Lopez, R.; Agrifoglio, G. *Inorg. Chem.* **1994**, *33*, 3177.
(7) Küsthardt, U.; Albach, R. W.; Kiprof, P. *Inorg. Chem.* **1993**, *32*, 1838.
(8) Oku, H.; Ueyama, N.; Kondo, M.; Nakamura, A. *Inorg. Chem.* **1994**, *33*, 209. Roberts, S. A.; Young, C. G.; Cleland, W. E., Jr.; Ortega, R. B.; Enemark, J. H. *Inorg. Chem.* **1988**, *27*, 3044. Harlan, E. W.; Berg, J. M.; Holm, R. H. *J. Am. Chem. Soc.* **1986**, *108*, 6992. Gheller, S. F.; Schultz, B. E.; Scott, M. J.; Holm, R. H. *J. Am. Chem. Soc.* **1992**, *114*, 6934.
(9) Schultz, B. E.; Holm, R. H. *Inorg. Chem.* **1993**, *32*, 4244.

0020-1669/96/1335-1273$12.00/0

Scheme 3

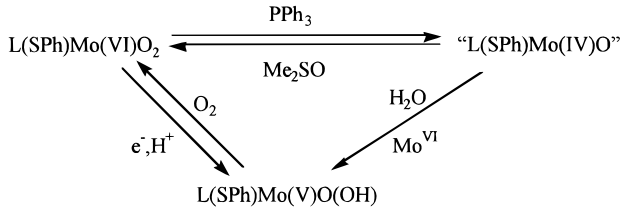

Mo(V) analogues, postulated in the reoxidation of the catalyst, have not been synthesized with the same success.[2,3] $Mo^{IV}O$ reacts with $Mo^{VI}O_2$ to form a μ-oxo dimer that inhibits the production of monomeric Mo(V). This dimerization is prevented in the enzyme by bulky substituents and the rigidity of the active site. Recently, at least two groups were able to synthesize monomeric Mo(V) analogues with the use of bulky ligands and donor solvents.[4,10]

With the use of the bulky hydrotris(3,5-dimethyl-1-pyrazolyl)-borate anion (L) ligand, Xiao et al.[4] were able to synthesize a model system which acts in a complete catalytic cycle. The key steps in this model system are shown in Scheme 3. The Mo(VI) species, $L(SPh)Mo^{VI}O_2$, is reduced with the substrate PPh_3, in DMF or MeCN, to form "$L(SPh)Mo^{IV}O$". This species is not seen directly but is trapped in pyridine as $L(SPh)Mo^{IV}O(py)$ or in CH_2Cl_2 as $L(SPh)Mo^{V}OCl$. In toluene, the Mo(IV) species interacts with the Mo(VI) species and dimerizes. In H_2O and in the presence of $L(SPh)Mo^{VI}O_2$, the Mo(IV) species reacts with the Mo(VI) species to form $L(SPh)Mo^{V}O(OH)$ most likely through the intermediate $L(SPh)Mo^{IV}O(OH_2)$. In completing the catalytic cycle, the Mo(V) species is oxidized by O_2 back to the original Mo(VI) species. Isotopic labeling studies show that the oxygen in the OH group of the Mo(V) species and one oxygen on the re-formed Mo(VI) species come from H_2O and not from the O_2.

The number of theoretical studies on oxo−molybdenum systems has been very limited. Previous work by Rappé and Goddard[11] suggests that the second oxygen, known as the spectator oxygen, plays an important role in the chemistry of complexes with cis oxygens. When both oxygens are oxo groups, each oxygen prevents the other oxygen from forming a formal triple bond with the metal center. But, with the addition of a substrate across one metal−oxo bond, the spectator oxygen (the oxygen not involved in the reaction) may form a triple bond with the metal center which stabilizes the product. Density functional[12] studies have been completed on $[MoCl_4O]^-$ and related complexes to interpret the UV−visible spectra. Semiempirical[10] and ab initio[10] studies completed on Mo(V) dioxo complexes predicted that the HOMO is composed of mainly Mo d character, a result which is consistent with the EPR spectra.

Here, we describe a theoretical model system based primarily on the synthetic model system of Xiao et al.[4] We use this system to determine details of the reaction mechanism by identifying the structures and energies of possible intermediates and transition states. Although the energetics for the entire reaction are studied, the main focus in this study is the transfer of the oxygen atom from the molybdenum center to the substrate and the subsequent displacement of the substrate oxide by water.

Development of the Model System

In our model system (see Figure 1), the hydrotris(3,5-dimethyl-1-pyrazolyl)borate anion, used to prevent the dimerization of Mo(V), was replaced with two amine groups and a SH^- group. The amine groups and SH^- group were fixed at 90° angles with respect to each other. Fixing the ligands mimicked the local steric effects associated with the bulky ligand used experimentally. In addition, using two amine groups and a SH^- group reproduced the charge, π-donor characteristics, and softness of the bulky ligand as well as the oxidation state of the metal. The SPh^- group was replaced with another SH^- ligand and placed at a right angle from both amine groups but 180° from the other SH^- group. These substitutions allowed C_{2v} and C_s symmetries to be used for most calculations. This ligand system is also very similar to the experimental model system of Holm and co-workers.[9]

In the first step of our model catalytic cycle (Scheme 4), trimethylphosphine approaches an oxygen atom attached to $(NH_3)_2(SH)_2Mo^{VI}O_2$. The phosphine extracts the oxygen to form trimethylphosphine oxide, and a water molecule enters the site vacated by the extracted oxygen atom. This process

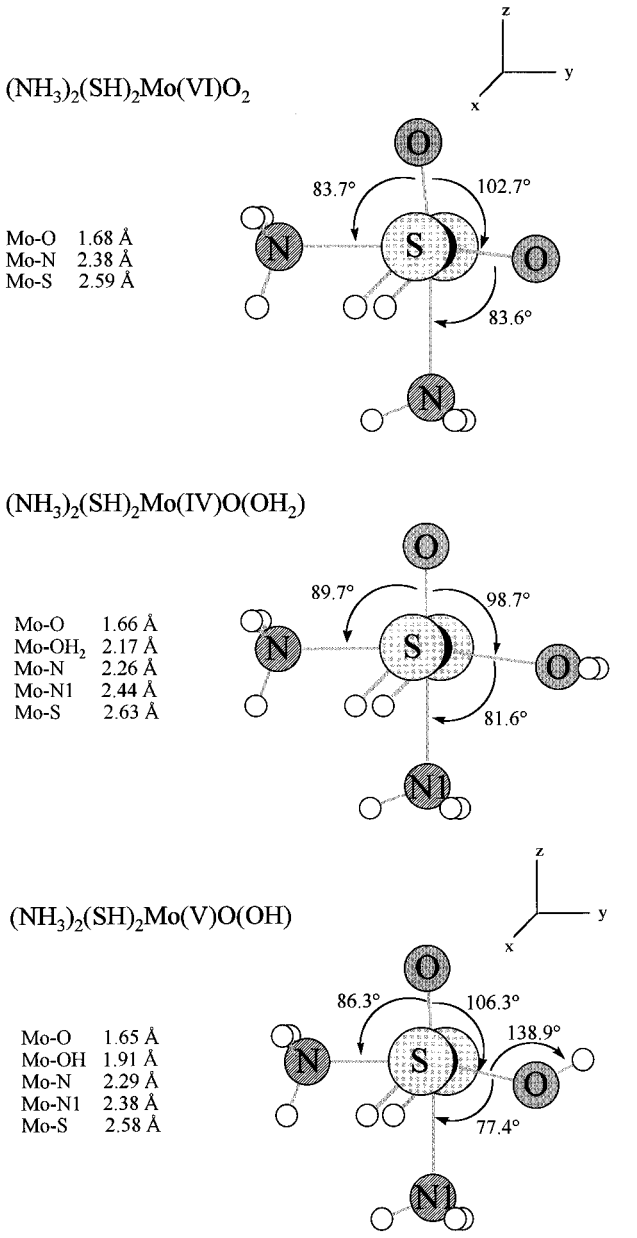

Figure 1. Geometries of $(NH_3)_2(SH)_2Mo^{VI}O_2$, $(NH_3)_2(SH)_2Mo^{IV}O(OH_2)$, and $(NH_3)_2(SH)_2Mo^{V}O(OH)$ optimized at the RHF (ROHF) level with a double-ζ basis set.

(10) Peng, G.; Nichols, J.; McCullough, E. A., Jr.; Spence, J. T. *Inorg. Chem.* **1994**, *33*, 2857.
(11) Rappé, A. K.; Goddard, W. A., III. *J. Am. Chem. Soc.* **1982**, *104*, 3287.
(12) Deeth, R. J. *J. Chem. Soc., Dalton Trans.* **1991**, 1895.

Scheme 4

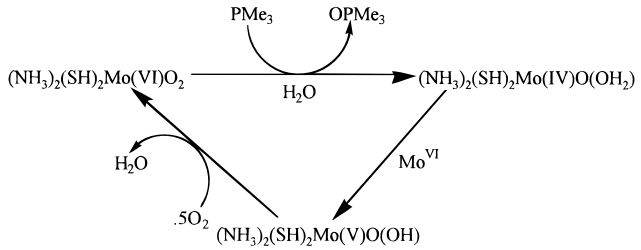

causes $(NH_3)_2(SH)_2Mo^{VI}O_2$ to be reduced to $(NH_3)_2(SH)_2Mo^{IV}O(OH_2)$. In the next step, $(NH_3)_2(SH)_2Mo^{IV}O(OH_2)$ is oxidized by a one-electron process to $(NH_3)_2(SH)_2Mo^{V}O(OH)$. Then, by another one-electron process, $(NH_3)_2(SH)_2Mo^{V}O(OH)$ is oxidized back to $(NH_3)_2(SH)_2Mo^{VI}O_2$. The cycle continues until all the phosphine is converted into phosphine oxide, which is the driving force of the reaction.

Theoretical Details

A comprehensive study comparing various levels of Møller−Plesset (MP) perturbation theory and other variational configuration interaction methods was recently completed for the oxo-transfer step in several simpler model systems.[13] From this study, we concluded that MP3 was the first reliable order of perturbation theory for the energies of the various oxo−molybdenum complexes involved in the catalytic cycle.

In the work described here, all geometries were optimized at the restricted Hartree−Fock (RHF) or open-shell RHF (ROHF) level. Zero-point-energy corrections which could be several kilocalories per mole have not been made. Approximate transition states were located by following an intrinsic reaction coordinate from reactant to intermediate and intermediate to product. Single-point MP3 calculations, restricted for closed shells and unrestricted for open shells, were performed for each optimized structure. The N−H bond lengths were fixed at 1.008 Å with a H−N−H bond angle of 107.3°. The S−H bond lengths were fixed at 1.345 Å, and the Mo−S−H bond angle was fixed at 93.3°. For trimethylphosphine and trimethylphosphine oxide, the C−H bonds were fixed at 1.134 Å and the P−C−H angles were fixed at 109.47°.

For each atom, except hydrogen, the core and valence electrons were divided, and ECPs were used for molybdenum (1s2s2p3s3p3d),[14a] oxygen (1s), nitrogen (1s), carbon (1s), sulfur (1s2s2p), and phosphorus (1s2s2p),[14b] while the valence electrons were described by a double-ζ basis set.[14] In addition, a polarization function of 0.340 was added to phosphorus to properly describe the hypervalent molecules containing phosphorus.[15] This polarization function is more important for P than for S because P is directly involved in the reaction.

All calculations were performed with the GAMESS-UK[16] and Gaussian92[17] packages at the Cornell National Supercomputer Facility (CNSF) on an IBM 3090-600VF, at the Supercomputer Center of Texas A&M University on a Cray Y-MP2/116, at the Supercomputer Center of Cray Research, Inc.,[18] Eagan, MN, on a Cray C-98-256Mw-8, and in our Chemistry Department on a Cray SMP and Silicon Graphics workstations.

Results and Discussion

Driving Force of the Reaction. Experimentally, the overall driving force for the reaction is the production of triphenylphosphine oxide from triphenylphosphine and oxygen, $PPh_3 + 0.5O_2 \rightarrow OPPh_3$, which has been measured to be exothermic by 67 kcal/mol.[3]

To decrease the number of atoms in the computational model, we first tried the replacement of the phenyl groups with hydrogen atoms. However, the calculated exothermicity was only 40 kcal/mol at the MP3 level. Since the energetics of the reaction $PH_3 + 0.5O_2 \rightarrow OPH_3$ did not satisfactorily replicate the reaction energy found experimentally for $PPh_3 + 0.5O_2 \rightarrow OPPh_3$, methyl groups were used in place of the hydrogens for the compututional model. Both trimethylphosphine and trimethylphosphine oxide were optimized in C_{3v} symmetry. For PMe_3, the P−C bond optimized at 1.89 Å, slightly longer than the electron diffraction value of 1.847 Å.[19] The P−O and P−C bonds for $OPMe_3$ optimized at 1.52 and 1.85 Å, respectively. These bond lengths are slightly larger than those found experimentally, 1.476 and 1.809 Å, respectively.[20] The optimized O−P−C angle (112.5°) was slightly less than found experimentally (114.4°). This reaction, $PMe_3 + 0.5O_2 \rightarrow OPMe_3$, was exothermic by 57.9 kcal/mol at the MP3 level, sufficiently close to the experimental system to make valid comparisons. In summary, the model phosphine must have a similar O−P bond energy for the calculated reaction profile to resemble the experimental one.

Geometries of the Model System. $(NH_3)_2(SH)_2Mo^{VI}O_2$ was optimized in C_{2v} symmetry (Figure 1). Although the Mo−O bonds are typical of bond lengths for Mo−O triple bonds,[21] the bonds formally have a bond order of 2.5 since both the p_y orbital of the top oxygen and the p_z orbital of the other oxygen compete for the same Mo d_{yz} orbital (Figure 2a). The optimized Mo−O bond lengths (1.68 Å) were slightly shorter than the Mo−O bond lengths (1.696 Å) found experimentally[22] for $MoO_2(^t$BuL-NS$)_2$, and the optimized O−Mo−O angle was smaller than the experimental one by 4.3°. Our theoretical Mo−S and Mo−N bond lengths in this model system were greater (0.172 Å) and shorter (0.031 Å), respectively, than those found experimentally in $MoO_2(^t$BuL-NS$)_2$, in which the sulfur and nitrogen lengths are quite different.

For the reduced (d^2) species with an oxygen vacancy, $(NH_3)_2(SH)_2Mo^{IV}O$, one must first determine which d orbitals are occupied (Figure 2b). The lowest-energy singlet state has both electrons in the a″ (Mo d_{xy}) orbital. Although occupation of other Mo d orbitals was considered, these alternative configurations were eliminated for the following reasons. Occupying the a′ (Mo d_{yz}) orbital would cause a repulsion between the electrons in the Mo d_{yz} orbital and the electrons in the p_y orbital of the top oxygen by preventing triple-bond formation. Furthermore, since the a′ (Mo d_{yz}) orbital is of the same symmetry as the lower-lying a′ (Mo $d_{x^2-y^2}$) orbital, standard SCF techniques would relax to the latter configuration. The a′ (Mo $d_{x^2-y^2}$) orbital remains higher in energy than the a″ (d_{xy}) orbital because it has substantial σ^* character. Occupying the a″ (d_{xz}) orbital would again cause a four-electron repulsion with the top oxygen, and again, the a″ (Mo d_{xz}) orbital would relax into the lower-lying a″ (Mo d_{xy}) singlet state. The lowest-energy

(13) Pietsch, M. A.; Couty, M.; Hall, M. B. *J. Phys. Chem.* **1995**, *99*, 16315.
(14))(a) Wadt, W. R.; Hay, J. H. *J. Chem. Phys.* **1985**, *82*, 299. (b) Stevens, W. J.; Basch, H.; Krauss, M. *J. Chem. Phys.* **1984**, *81*, 6026.
(15) Huzinaga, S.; Andzelm, J.; Klobukowski, M.; Radzio-Andzelm, E.; Sakai, Y.; Tatewaki, H. *Gaussian Basis Sets for Molecular Calculations*; Elsevier: Amsterdam, 1984.
(16) Dupuis, M.; Spangler, D.; Wendolowski, J. *NRCC Software Catalog*; Vol. 1, Program No. QG01 (GAMESS). Guest, M. F.; Fantucci, P.; Harrison, R. J.; Kendrick, J.; van Lenthe, J. H.; Schoeffel, K.; Sherwood, P. *GAMESS-UK*; CSF Ltd., 1993.
(17) Frisch, M. J.; Trunks, G. W.; Head-Gordon, M.; Gill, P. M. W.; Wong, M. W.; Foresman, J. B.; Johnson, B. G.; Schlegel, H. B.; Robb, M. A.; Replogle, E. S.; Gomperts, R.; Andres, J. L.; Raghavachari, K.; Binkley, J. S.; Gonzales, C.; Martin, R. L.; Fox, D. J.; Defrees, D. J.; Baker, J.; Stewart, J. J. P.; Pople, J. A. *Gaussian 92*, Revision B; Gaussian Inc.: Pittsburgh, PA, 1992.
(18) We thank Chris Hempel and Cray Research Inc. for providing the opportunity of using the Cray C-98-512Mw-8.
(19) Bartell, L. S.; Brockway, L. O. *J. Chem. Phys.* **1960**, *32*, 512.
(20) Wilkins, C. J.; Hagen, K.; Hedberg, L.; Shen, Q.; Hedberg, K. *J. Am. Chem. Soc.* **1975**, *97*, 6352.
(21) Mayer, J. M. *Inorg. Chem.* **1988**, *27*, 3899. Spiro, G. *Molybdenum Enzymes*, Wiley-Interscience: New York, 1985.
(22) Schultz, B. E.; Gheller, S. F.; Muetterties, M. C.; Scott, M. J.; Holm, R. H. *J. Am. Chem. Soc.* **1993**, *115*, 2714.

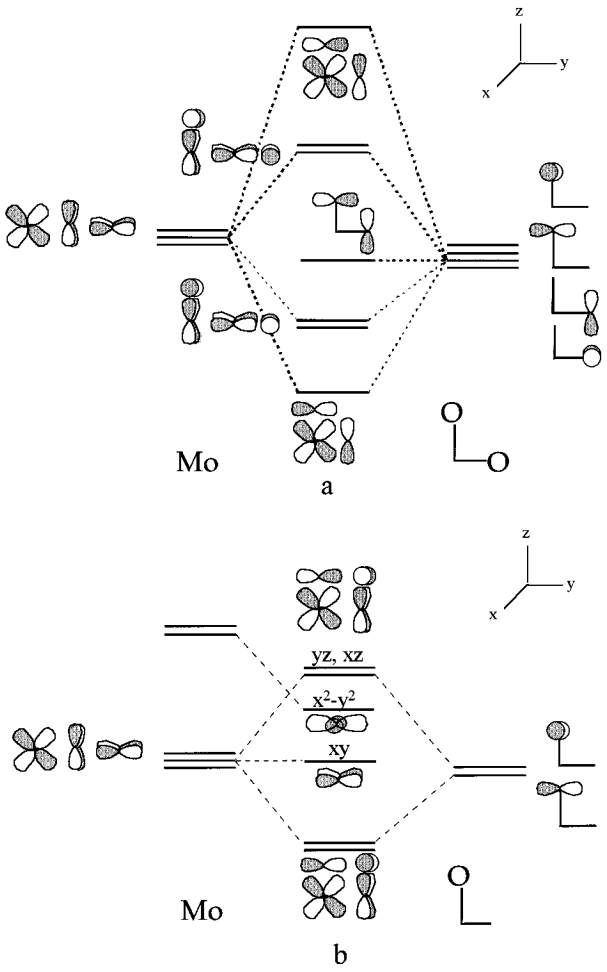

Figure 2. (a) Molecular orbital diagram of the interaction between the p orbitals of the oxygen atoms and the molybdenum d_{xy}, d_{xz}, and d_{yz} orbitals. The Mo d_{yz} orbital is shared between the p_y ofbital of the top oxygen and the p_z orbital of the side oxygen. The Mo d_{xy} orbital bonds with the p_x orbital of the side oxygen, and the Mo d_{xz} orbital bonds with the p_x orbital of the top oxygen. The orbitals are filled up to the nonbonding oxygen orbital. (b) Molecular orbital diagram after one oxygen is removed. The nonbonding oxygen orbital is replaced with a nonbonding (with respect to O) Mo d orbital.

triplet state has one electron in the a′ ($d_{x^2-y^2}$) orbital and one electron in the a″ (d_{xy}) orbital. In order to determine whether the ground state is a singlet or a triplet, the two configurations were used in a partial geometry optimization (all ligand angles were fixed at a 90° angle). In the singlet state, the Mo−O bond distance optimized to 1.65 Å, while in the triplet state, the distance elongated to 1.71 Å. Next, configuration interaction calculations with single and double excitations (CISD) were performed on the optimized singlet and triplet. At this level, the singlet was lower in energy than the triplet but only by about 1 kcal/mol. However, access to the triplet-state surface is formally forbidden by symmetry and we will assume that the reaction will remain on the singlet surface.

In the final geometry optimizations, $(NH_3)_2(SH)_2Mo^{IV}O$ was optimized in C_s symmetry as a singlet state with the two d electrons in the a″ (d_{xy}) orbital without any constraints on the N−Mo−O bond angles. The Mo−O bond optimized to 1.65 Å, which is 0.03 Å shorter than the Mo−O bond optimized in $(NH_3)_2(SH)_2Mo^{IV}O_2$. We have not considered the ligand rearrangement observed in Holm's model because Xiao et al.'s tridentate ligand system prevents such a rearrangement.

$(NH_3)_2(SH)_2Mo^{IV}O(OH_2)$, where water now replaces the vacant site, was optimized in C_s symmetry (Figure 1). The two d electrons were again placed in a Mo a″ (d_{xy}) orbital, consistent

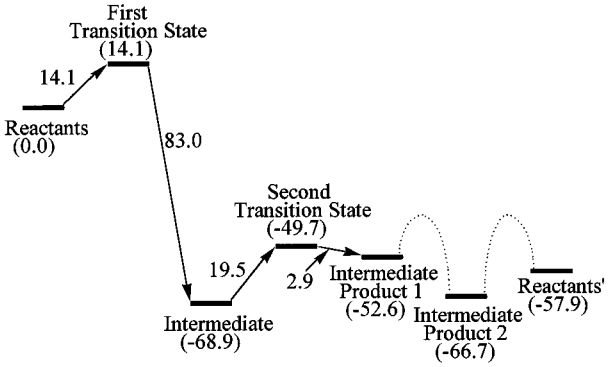

Figure 3. Relative energies of the model system with respect the reactants. The dotted line indicates that the path between the intermediate products and reactants′ was not determined. Reactants: $2(NH_3)_2(SH)_2Mo^{VI}O_2 + PMe_3 + H_2O + 0.5O_2$. Intermediates: $(NH_3)_2(SH)_2Mo^{VI}O_2 + (NH_3)_2(SH)_2Mo^{IV}O(OPMe_3) + H_2O + 0.5O_2$. Intermediate product 1: $(NH_3)_2(SH)_2Mo^{VI}O_2 + (NH_3)_2(SH)_2Mo^{IV}O(OH_2) + OPMe_3 + 0.5O_2$. Intermediate product 2: $2(NH_3)_2(SH)_2Mo^{V}O(OH) + OPMe_3 + 0.5O_2$. Reactants: $2(NH_3)_2(SH)_2Mo^{VI}O_2 + OPMe_3 + H_2O$.

with the $(NH_3)_2(SH)_2Mo^{IV}O$ results. Occupation of the Mo d_{xy} orbital allows the formation of a molybdenum−oxo triple bond with a length of 1.66 Å. The Mo−OH_2 bond is considerably longer at 2.17 Å. The nitrogens show a strong trans influence with the Mo−N bond (2.44 Å) trans to the oxo group being longer than the Mo−N bond (2.26 Å) trans to the OH_2 group.

$(NH_3)_2(SH)_2Mo^{V}O(OH)$ was optimized in C_s symmetry (Figure 1). The unpaired d electron was again placed in the a″ (d_{xy}) orbital to minimize repulsion with the top oxygen. Although the Mo−OH bond (1.91 Å) is longer than the Mo−O bond (1.68 Å) of $(NH_3)_2(SH)_2Mo^{VI}O_2$, it is shorter than the Mo−OH_2 bond (2.17 Å) in $(NH_3)_2(SH)_2Mo^{IV}O(OH_2)$. Again, the trans influence is seen with the Mo−N bond length (2.38 Å) trans to the oxo group being greater than the Mo−N bond length (2.29 Å) trans to the OH group.

Energetics of the Model System. The extraction of the oxygen atom from $(NH_3)_2(SH)_2MoO_2$ by PMe_3 and the insertion of H_2O for the overall reduction of Mo(VI) to Mo(IV) are calculated to be exothermic by 52.6 kcal/mol (Scheme 4 and Figure 3). During the oxidation of $(NH_3)_2(SH)_2Mo^{IV}O(OH_2)$ to $(NH_3)_2(SH)_2Mo^{V}O(OH)$, an additional 14.1 kcal/mol of energy is released. The final step, oxidation of $(NH_3)_2(SH)_2Mo^{V}O(OH)$ to $(NH_3)_2(SH)_2Mo^{VI}O_2$, is endothermic by 8.8 kcal/mol. The latter energy difference, oxidation of $(NH_3)_2(SH)_2Mo^{V}O(OH)$ to $(NH_3)_2(SH)_2Mo^{VI}O_2$, may be overestimated since the energy of $(NH_3)_2(SH)_2Mo^{V}O(OH)$ was computed with unrestricted MP3 while the energy for $(NH_3)_2(SH)_2Mo^{VI}O_2$ was computed with restricted MP3. The same argument can be made for the oxidation of $(NH_3)_2(SH)_2Mo^{IV}O(OH_2)$ to $(NH_3)_2(SH)_2Mo^{V}O(OH)$. This cycle is of course calculated for the gas-phase species. Because of the large dipole moment of $OPMe_3$ compared to PMe_3, solvent effects will stablize all of the species beyond the intermediate. This effect coupled with the previous overestimation of the stability of the Mo(V) species will generate a progressively exothermic cycle. The overall reaction, $PMe_3 + 0.5O_2 \rightarrow OPMe_3$, is exothermic by 57.9 kcal/mol.

The Oxo-Transfer Step. PMe_3 approaches an oxygen atom of $(NH_3)_2(SH)_2Mo^{VI}O_2$ at approximately a 130° Mo−O−P angle and a 90° O−Mo−O−P dihedral angle. The phosphorus approaches at this dihedral angle since the Mo d_{xy}−O p_y and Mo d_{xz}−O p_x antibonding combinations are lower in energy than the Mo d_{yz}−O p_z−O p_y (Figure 2a). As the phosphorus comes closer to the oxygen, the two electrons currently forming the Mo d_{xy}−O p_x bond transfer to the Mo d_{xy} orbital, allowing the

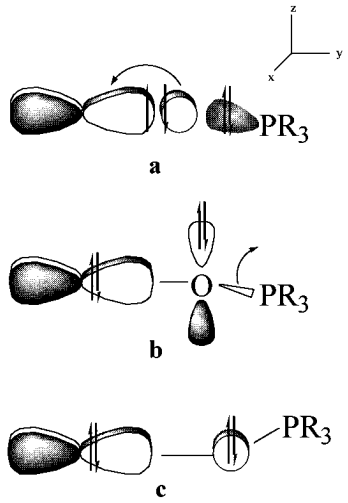

Figure 4. Orbital representation of the first transition state. (a) As the phosphine approaches the oxygen atom, the electron pair forming a Mo−O bond transfers to the Mo d_{xy} orbital. The O p_z orbital is not shown. (b) An O−P bond is formed, and the OPR_3 group begins to rotate upward. The O p_z is shown. (c) Once the OPR_3 rotates 90°, the O p_z orbital becomes the O p_x orbital, which causes electron−electron repulsion between the molybdenum and oxygen, weakening the Mo−O bond.

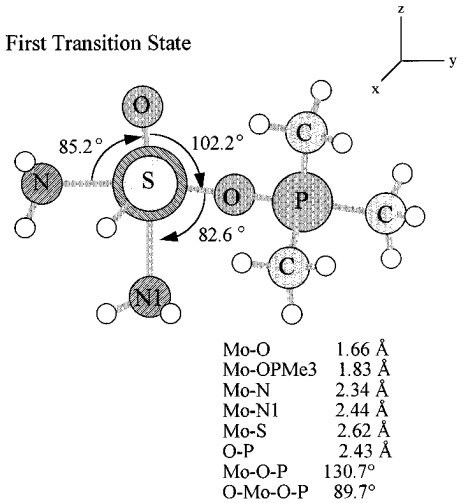

Figure 5. Geometry of the transition state, $(NH_3)_2(SH)_2Mo^{IV}O(OPMe_3)$, optimized at the RHF level with a double-ζ basis set.

phosphorus lone pair to form a bond with the O p_x orbital (Figure 4a). The transition state barrier at the MP3 level for this process is 14.1 kcal/mol (Figure 3). At the transition state, the lengths of the weakened Mo−O bond and forming O−P bond are 1.83 and 2.43 Å, respectively, and the P−O−Mo−O dihedral angle is 89.7° (Figure 5). The remaining oxo group shortens slightly from 1.68 Å in $(NH_3)_2(SH)_2Mo^{VI}O_2$ to 1.66 Å at the transition state. Once the O−P bond is formed (Figure 4b), the $OPMe_3$ ligand rotates, decreasing the O−Mo−O−P dihedral angle; this motion rotates the O p_z orbital and breaks the remains of the Mo d_{yz}−O p_z (π) bond (Figure 4c). As this rotation occurs, the Mo−$OPMe_3$ bond lengthens, and the O−P bond shortens. When the O−Mo−O−P dihedral angle reaches 0°, the occupied O p_z orbital has become an O p_x orbital, and electron−electron repulsion between the O p_x pair orbital and the electron pair in the Mo d_{xy} orbital lengthens the Mo−$OPMe_3$ bond (Figure 4c). This process leads to the intermediate species, $(NH_3)_2(SH)_2Mo^{VI}O(OPMe_3)$.

This intermediate, $(NH_3)_2(SH)_2Mo^{VI}O(OPMe_3)$, was optimized in C_1 symmetry (Figure 6) with the two electrons remaining in the d_{xy} orbital. Although the species was optimized

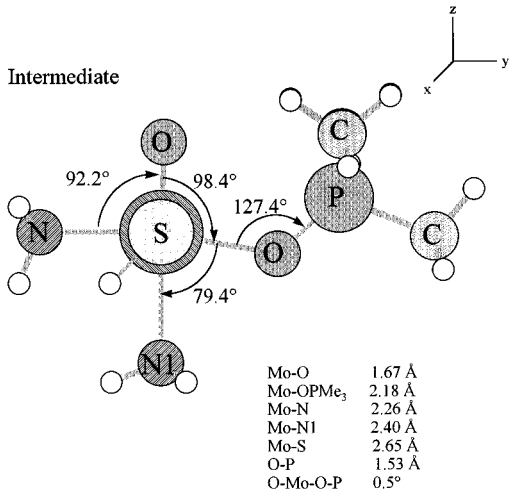

Figure 6. Geometry of the intermediate, $(NH_3)_2(SH)_2Mo^{IV}O(OPMe_3)$, optimized at the RHF level with a double-ζ basis set.

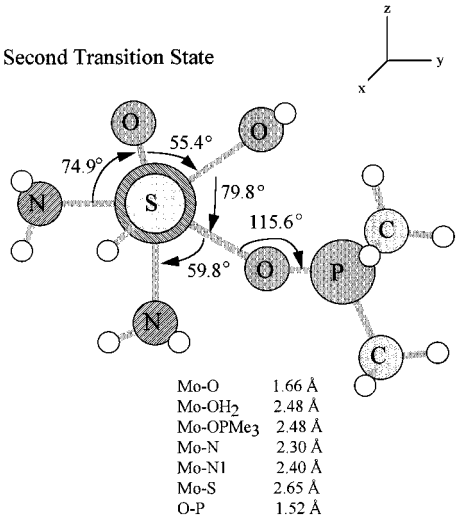

Figure 7. Geometry of the associative transition state, $(NH_3)_2(SH)_2$-$Mo^{IV}O(OPMe_3)(OH_2)$, optimized at the RHF level with a double-ζ basis set.

in C_1 symmetry, the O−Mo−O−P dihedral angle optimized to 0.4°, nearly C_s symmetry. The trans influence can also be seen here in the Mo−N bond distances. At the intermediate geometry, the O−P bond has formed and the oxygen has a lone pair forming a dative bond with the molybdenum center. The Mo−$OPMe_3$ bond distance of 2.18 Å is similar to that found for the Mo−OH_2 bond. This intermediate is 68.9 kcal/mol lower in energy than $(NH_3)_2(SH)_2MoO_2 + PMe_3$ (Figure 3). Rotating the O−Mo−O−P dihedral angle back to 90° in the intermediate increases the energy by 4 kcal/mol (RHF) and increases the Mo−$OPMe_3$ distance by 0.02 Å.

After the intermediate forms, $OPMe_3$ dissociates from the molybdenum center and water attaches at the site vacated by $OPMe_3$ to form $(NH_3)_2(SH)_2MoO(OH_2)$. Two possible reaction mechanisms could be operational for the exchange: (i) a dissociative mechanism where $OPMe_3$ leaves before OH_2 enters; (ii) an associative mechanism where a concerted exchange occurs between $OPMe_3$ and OH_2. Since $(NH_3)_2(SH)_2Mo^{IV}O +$ $OPMe_3$ separated at infinite distance is 56.5 kcal/mol higher in energy than the intermediate, the dissociative mechanism was eliminated from further consideration. Thus, the associative mechanism, concerted exchange, was examined. The transition state for the associative mechanism is only 19.2 kcal/mol higher in energy than the intermediate (Figure 3). The transition state structure (Figure 7) has both Mo d electrons in the d_{xy} orbital.

The O−P bond (1.52 Å) is fully formed with both OH_2 and $OPMe_3$ approximately 2.59 Å away from the molybdenum center.

Conclusion

The energy profile for our model system is in qualitative accord with what is known experimentally about these systems. Our barrier of 14 kcal/mol is consistent with the $\Delta H^{\ddagger}$ measurement of 10−17 kcal/mol for oxo transfer to various phosphines.[9] The direction of approach of the substrate is critical to maximizing the value of the spectator oxygen in assisting the reaction. The subsequent rotation of the substrate to form the intermediate weakens the substrate oxide's bond to the metal center in preparation for its release. The release of the substrate oxide product proceeds by an associative displacement reaction.

Acknowledgment. We thank the Robert A. Welch Foundation (Grant A-648) and the National Science Foundation (Grants CHE 91-13634 and 94-23271) for financial support. We also thank Drs. M. F. Guest and P. Sherwood for providing the GAMESS package of programs and Dr. John Enemark for bringing this problem to our attention and for helpful discussions of the major issues.

IC951044P